Ultrasonics Sonochemistry 100 (2023) 106612

Contents lists available at ScienceDirect

Ultrasonics Sonochemistry

journal homepage: www.elsevier.com/locate/ultson

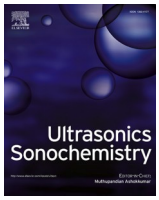

Quantitation and evaluation of NO_2^-, NO_3^-, and H_2O_2 in the sonolysis of aqueous NaOH solution under air and air-Ar mixture: Effects of solution temperature, ultrasonic power, and ratio of gas mixture

Kenji Okitsu [a,b,*], Riki Kunichika [b], Shota Asada [b]

[a] Graduate School of Sustainable System Sciences, Osaka Metropolitan University, 1-1 Gakuen-cho, Sakai, Osaka 599-8531, Japan
[b] Graduate School of Humanities and Sustainable System Sciences, Osaka Prefecture University, 1-1 Gakuen-cho, Sakai, Osaka 599-8531, Japan

ARTICLE INFO

Keywords:
N_2 oxidation
NO_3^-
NO_2^-
H_2O_2
Solution temperature
Ultrasonic power
Air–argon mixture

ABSTRACT

When an aqueous solution containing dissolved air is sonicated, H_2O_2, HNO_2, and HNO_3 are formed. This is a result of the formation of active bubbles with extremely high-temperature and high-pressure. The yields of H_2O_2, NO_2^-, and NO_3^- are representative indexes for understanding the chemical effects of ultrasonic cavitation in water. However, these yields often vary under the acidic conditions caused by sonication. In this study, we measured the yields of H_2O_2, NO_2^-, and NO_3^- in the presence of NaOH, which suppresses the reaction between NO_2^- and H_2O_2 and prevents the formation of NO_3^- in a bulk solution. Therefore, the yields obtained should correspond to the actual yields just after bubble collapse, directly reflecting the chemical effects of the active bubbles themselves. It was confirmed that the yields of NO_2^- and NO_3^- decreased, while the ratio of [NO_3^-] to [NO_2^-] ([NO_3^-]/[NO_2^-] ratio) increased with increasing solution temperature, suggesting that the temperature and pressure in collapsing bubbles decreased with an increase in the solution temperature. Ultrasonic power clearly affected the yields of NO_2^- and NO_3^-, but it did not affect the [NO_3^-]/[NO_2^-] ratio, suggesting that 1) the quality of the active bubbles did not change largely with increasing ultrasonic power, and 2) the quantity related to the number and/or size of active bubbles increased with increasing ultrasonic power up to a certain power. Additionally, the effects of the ratio of air to Ar on the yields of NO_2^-, NO_3^-, and H_2O_2 were investigated. These yields could be affected not only by the bubble temperature but also by the concentration of reactants and intermediates inside the collapsing bubbles. The chemical reactions are quite complex, but these yields could be valuable analytical tools for understanding the quantity and quality of active bubbles.

1. Introduction

Transient microbubbles with extremely high temperatures and pressures are generated during ultrasonic cavitation in water. These bubbles have been actively studied in various fields such as synthesis of nanostructured materials, degradation of hazardous chemicals, and sonodynamic therapy. During the sonolysis of water, OH and H radicals are primarily formed [1,2] and some of the OH radicals recombine to form H_2O_2 [3,4]. The yields of H_2O_2 and/or OH radicals are representative indexes for understanding the chemical effects of ultrasonic cavitation. Thus, these yields have been measured under various experimental conditions, including parameters such as ultrasonic power [3,5,6,7], ultrasonic frequency [3,6,8,9,10,11,12], solution temperature [6,7,9,10], type of dissolved gas [4,8,9,13,14], pressure of dissolved gas [5], gas saturation and sparging system [9,14], solution mixing [9,15,16], solution volume [3,5,7], liquid height [11], and solution pH [7,17]. The effects of additives such as organic compounds [18], inorganic salts [19], particles [12], and micron-sized air bubbles [20,21] have also been investigated. In some cases, the yields are normalized by the applied ultrasonic power and/or solution volume and these values are referred to as the sonochemical efficiency [3,7,11,16]. Despite active analysis of these yields and efficiencies under various conditions, the characteristics of active bubbles remain unclear because of the complex nature of ultrasonic cavitation, which can be influenced by multiple factors even when only one parameter is altered.

When an aqueous solution containing dissolved air is irradiated by ultrasound, active bubbles are generated and N_2 oxidizes to form NO_2^- and NO_3^-. Therefore, the yields of NO_2^- and NO_3^- serve as additional

* Corresponding author at: Graduate School of Sustainable System Sciences, Osaka Metropolitan University, 1-1 Gakuen-cho, Sakai, Osaka 599-8531, Japan.
E-mail address: okitsu@omu.ac.jp (K. Okitsu).

https://doi.org/10.1016/j.ultsonch.2023.106612
Received 31 May 2023; Received in revised form 15 September 2023; Accepted 20 September 2023
Available online 23 September 2023

representative indexes to understand the chemical effects of ultrasonic cavitation [22–28]. We recently reported the possibility of using NO_2^- and NO_3^- as probes to investigate temperature- and pressure-dependent reactions. This approach aims to improve our understanding of the physicochemical properties of collapsing air bubbles [22]. Although N_2 oxidation and water decomposition have been actively studied for a long time, the characteristics and number of active bubbles, as well as their chemical effects, have not yet been sufficiently clarified. In this study, we discuss these unclear points by measuring the actual yields of NO_2^-, NO_3^-, and H_2O_2 just after bubble collapse. The yields and ratios of NO_2^- and NO_3^- formed under various experimental conditions, including different solution temperatures, ultrasonic powers, and gas mixtures with Ar, were compared. In particular, the bubble temperature attained during collapse, the number of active bubbles, and their chemical effects were evaluated to understand the characteristics of the active bubbles. In multi-bubble cavitation, when the ultrasonic power increases, it is generally considered that the quality related to the bubble temperature and quantity related to the number and/or size of the active bubbles change simultaneously, so that it has been difficult to distinguish the effects of these two factors. The present study is the first one to discuss the quality and quantity of the active bubbles by using experimental results of NO_2^- and NO_3^-.

2. Experimental

All the water used in the experiments was treated using a Millipore system (Milli-Q). Ultrasonic irradiation was performed using a 65 mm ϕ oscillator (Kaijo; Lot. No. 00102, Japan) and an ultrasonic generator (Kaijo 4021 type; Lot. No. 11EA00103, Japan; frequency: 200 kHz; nominal maximum power: 200 W). The details of the irradiation setup have been described in previous studies [29]. A cylindrical reaction vessel (inner diameter: 50 mm) was mounted such that the flat bottom of the vessel was 4.0 mm away from the top of the oscillator, where 4.0 mm was the optimum distance, which approximately corresponded to the half-wavelength of the ultrasound of 200 kHz [29]. Water containing dissolved air (60 mL) in the presence of NaOH (1.0 mM) was sonicated in a water bath maintained at 5, 10, 15, 20, 25, or 30 °C using a cold-water circulation system (TAITEC CL–150R). The reaction vessel remained open to the surrounding air during irradiation, and the effects of ultrasonic power and solution temperature were investigated (Figs. 1–3). For the experiments shown in Figs. 4–7, air, Ar, or a mixture of both gases was introduced into the sample solutions via a bubbling process. This process was carried out in a water bath at a total flow rate of 200 mL/min using a silicon tube. Prior to the experiments, the gas flow was initially directed through the tube for a duration of 30 min to eliminate any residual air or gas in the reaction system. Subsequently, the gas was passed through the tube for 60 min. The rates of the gas flows were controlled to make a desired gas mixture: the volume percentage of gaseous phase was controlled. The reaction vessel was sealed after gas bubbling, and sonication was performed under closed conditions (Figs. 4–7). The ultrasonic power applied to the sample solution (60 mL) was measured using a calorimetric method [30], where a K-type thermocouple (As One, DS-K 1.0 × 200, Japan; sheath diameter: 1.0 mm, sheath length: 200 mm) and data logger (midi LOGGER GL220, Graphtec, Japan; sampling time: 100 msec) were used. In this study, the calorimetric powers of 3.3 (power dial of the ultrasonic generator 2), 7.4 (power dial 4), 10.3 (power dial 6), 13.2 (power dial 8), and 15.0 W (power dial 10) were used for ultrasonic irradiation. The data as a function of irradiation time is shown in the Supplementary data (Fig. S1). The average obtained by three irradiation experiments for 60 sec was used to calculate the calorimetric powers. In this study, the acoustic intensity (I) was 0.17, 0.38, 0.52, 0.67, 0.76 W/cm^2, respectively, which was calculated from the calorimetric power by dividing the bottom surface area of the reaction vessel. The value of I is related to the acoustic pressure amplitude (P_a) as follows: $I = P_a^2/2\rho c$, where ρ is the density of a liquid and c is the sound velocity [31]. This equation

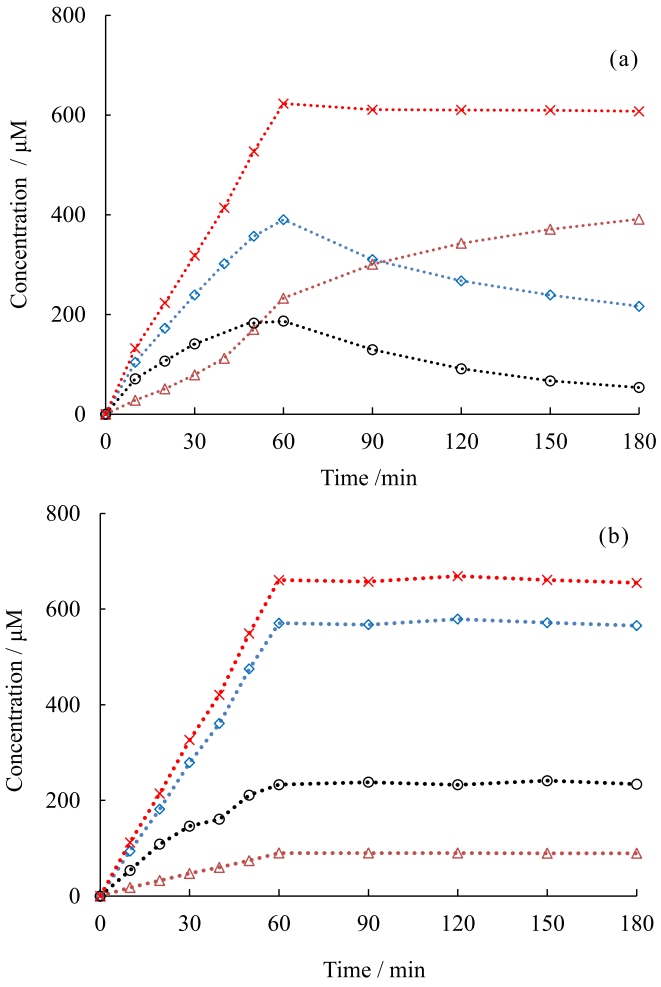

Fig. 1. Changes in concentrations of NO_2^-(◇), NO_3^-(△), H_2O_2 (○), and sum of NO_2^- and NO_3^-(×) with irradiation and with standing time after irradiation in the absence (a) and presence (b) of NaOH. Ultrasonic power turned off at 60 min. Ultrasonic power: 10.3 W, solution temperature: 20 °C.

indicates that the acoustic pressure amplitude increases with increasing acoustic intensity. In some parts in this paper, we use the term of the ultrasound power of calorimetric power which is related to a kind of the acoustic pressure amplitude.

After irradiation, the solution was sampled through a silicone rubber septum using a syringe and placed in a vial. The concentrations of NO_2^- and NO_3^- were measured by ion chromatography (IC, Metrohm 761 Compact IC, Switzerland). The IC analysis conditions were as follows: the separation column was Shodex IC SI-90 4E (Japan), and the eluent was a mixture of aqueous Na_2CO_3 (1.8 mM) and $NaHCO_3$ (1.7 mM) solution at a flow rate of 1.0 mL/min. The concentration of H_2O_2 was measured using the KI colorimetric method [32], using a UV–visible spectrophotometer (Shimadzu UV-2450, Japan): aqueous $KHC_8H_4O_4$ (potassium hydrogen phthalate, 0.10 M) solution labeled as solution A and a mixture of aqueous KI (0.40 M), NaOH (0.050 M), and $(NH_4)_6Mo_7O_{24}$ (hexaammonium heptamolybdate, 1.6×10^{-4} M) solution labeled as solution B were prepared, respectively. 2.0 mL of solution A and 2.0 mL of solution B were added to 1.0 mL of the sample solution in this order, and then the absorption spectrum of the mixed solution was measured.

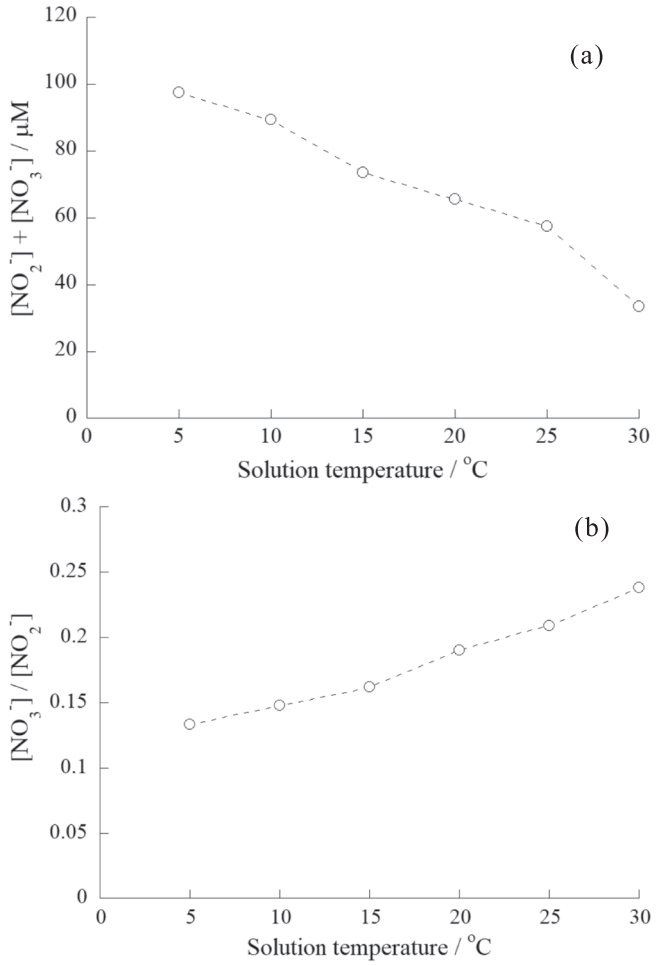

Fig. 2. (a)Effect of solution temperature on the sum of the yield of NO_2^- and NO_3^-. (b) Effect of solution temperature on the NO_3^-/NO_2^- ratio. Concentration of NaOH: 1.0 mM, sonication time: 5.0 min, ultrasonic power: 10.3 W.

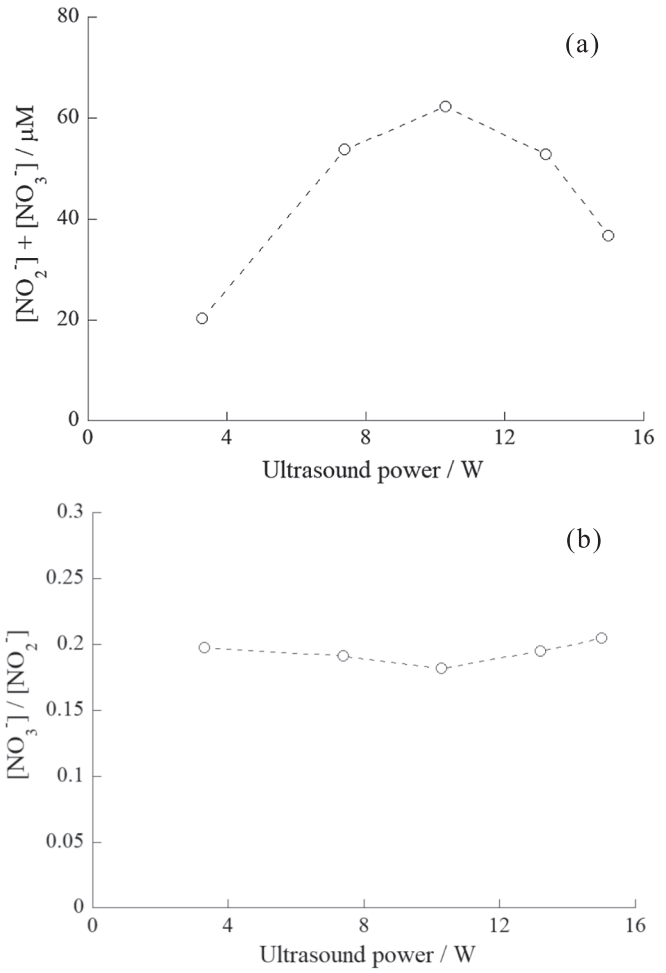

Fig. 3. (a) Effect of ultrasonic power on the sum of the yield of NO_2^- and NO_3^-. (b) Effect of ultrasonic power on the NO_3^-/NO_2^- ratio. Concentration of NaOH: 1.0 mM, sonication time: 5.0 min, solution temperature: 20 °C.

3. Results and discussion

3.1. Effect of NaOH

Fig. 1a and b show the variation in the concentrations of NO_2^-, NO_3^-, and H_2O_2 during the sonolysis of water containing dissolved air in the absence and presence of NaOH, respectively. The concentrations of NO_2^-, NO_3^-, and H_2O_2 increased with sonication time. These formations were caused by the generation of microbubbles with extremely high temperatures and pressures and then oxidation of N_2 via the Zeldovich and extended Zeldovich mechanisms [25,26,28,33,34]. Typical reaction equations are as follows:

$$H_2O \rightarrow OH + H \quad (1)$$

$$2OH \rightarrow H_2O_2 \quad (2)$$

$$H + O_2 \rightarrow OOH \quad (3)$$

$$2OOH \rightarrow H_2O_2 + O_2 \quad (4)$$

$$O_2 \rightarrow 2O \quad (5)$$

$$N_2 + O \rightarrow NO + N \quad (6)$$

$$N + O_2 \rightarrow NO + O \quad (7)$$

$$N + OH \rightarrow NO + H \quad (8)$$

After NO formation, NO_2, N_2O_3, HNO_2, and HNO_3 were formed as follows:

$$2NO + O_2 \rightarrow 2NO_2 \quad (9)$$

$$NO + OOH \rightarrow NO_2 + OH \quad (10)$$

$$NO + NO_2 \rightarrow N_2O_3 \quad (11)$$

$$NO + O \rightarrow NO_2 \quad (12)$$

$$NO + OH \rightarrow HNO_2 \quad (13)$$

$$NO_2 + OH \rightarrow HNO_3 \quad (14)$$

$$N_2O_3 + H_2O \rightarrow 2HNO_2 \quad (15)$$

$$2NO_2 + H_2O \rightarrow HNO_2 + HNO_3 \quad (16)$$

It can be seen in Fig. 1a that the concentrations of NO_2^-, NO_3^-, and H_2O_2 increased curvilinearly with irradiation time in the absence of NaOH. However, after the irradiation was stopped at 60 min, the concentrations of NO_2^- and H_2O_2 decreased with standing time, whereas the concentration of NO_3^- continued to increase. Furthermore, the combined concentration of NO_2^- and NO_3^- displays a linear increase during irradiation and then remains constant during the standing period without irradiation. As the ultrasonic irradiation of air-dissolved water makes the solution acidic [22], Fig. 1a shows that NO_2^- and H_2O_2 undergo a

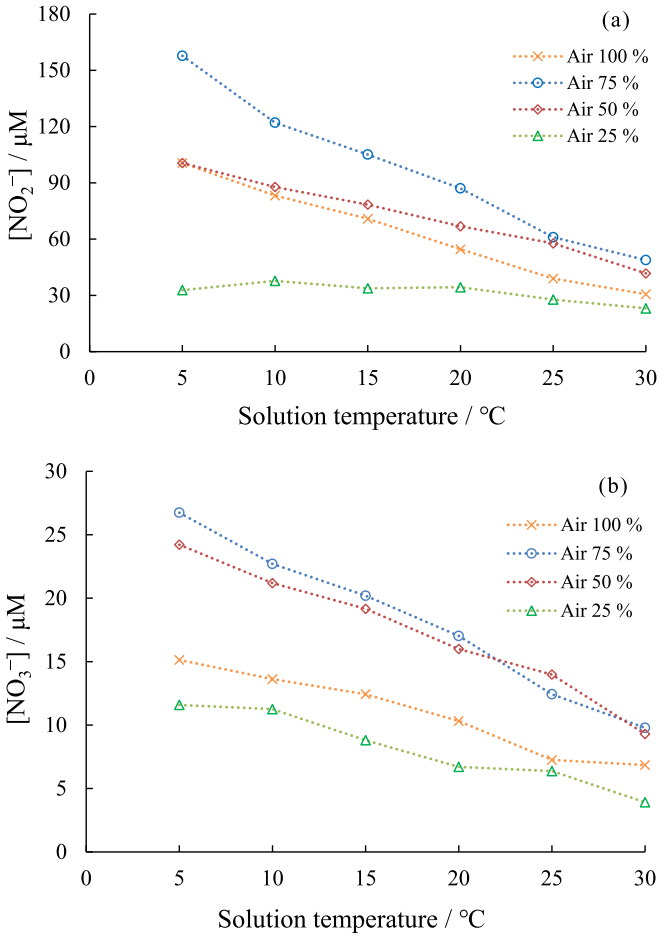

Fig. 4. Effect of solution temperature on the yield of (a) NO_2^- and (b) NO_3^- at different air-Ar ratio. (×): air 100%, (○) air 75%, (◇): air 50%, (△): air 25%. Concentration of NaOH: 1.0 mM, sonication time: 5.0 min, ultrasonic power: 10.3 W.

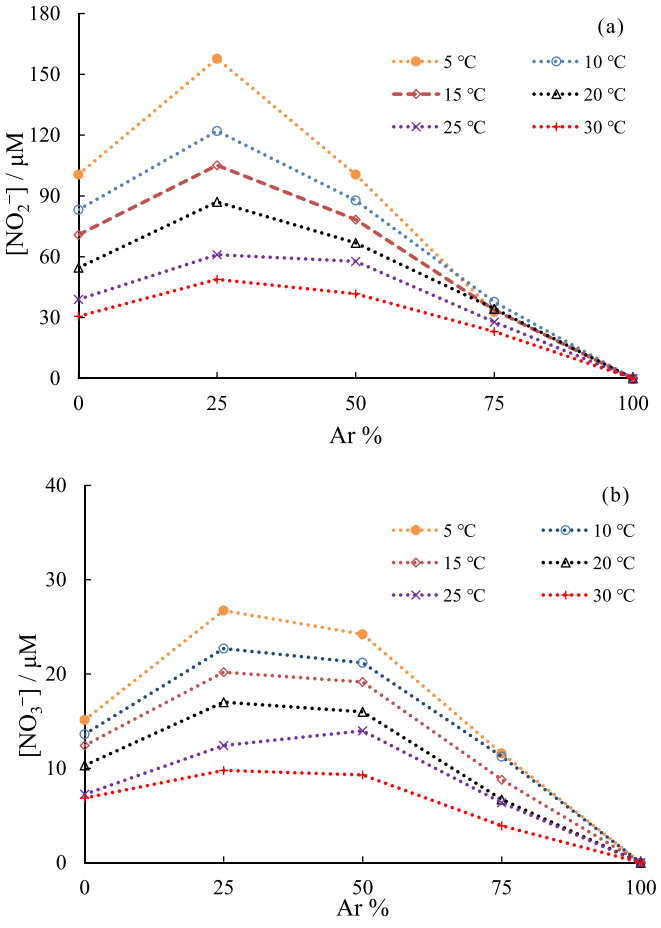

Fig. 5. Effect of Ar percentage in gas mixture on the yield of (a) NO_2^- and (b) NO_3^- at different solution temperature. Concentration of NaOH: 1.0 mM, sonication time: 5.0 min, ultrasonic power: 10.3 W.

redox reaction in the acidic solution to form NO_3^-, as shown in Eq. (17), both during the irradiation period and subsequent standing period without irradiation.

$$NO_2^- + H_2O_2 \rightarrow NO_3^- + H_2O \quad (17)$$

where above sentences and Eq. (17) are described without considering pK_a of HNO_2 (pK_a = 3.23 [35]) and HNO_3 (pK_a = − 1.8 [36]).

On the other hand, in Fig. 1b, the concentrations of NO_2^-, NO_3^-, and H_2O_2 increase linearly during irradiation in the presence of NaOH. In addition, these concentrations do not change during the standing period without irradiation. These results indicate that Eq. (17) was suppressed in the presence of NaOH. According to the report by Damschen and Martin [35], the progress of Eq. (17) needs H^+. It was also confirmed that the presence of acid promotes Eq. (17) in our study. In Supplementary data, the effects of acid and alkali on the progress of Eq. (17) were investigated and the results are shown in Figs. S2 and S3.

There are many reports on the yields of NO_2^-, NO_3^-, and H_2O_2 formed by ultrasonic irradiation [22–28]. However, in an uncontrolled pH aqueous solution, these yields may include some experimental errors under the following conditions: 1) when the yield of NO_2^- or NO_3^- is high, 2) when the irradiation time is long, 3) when it takes a long time to analyze the solution after the irradiation, and 4) when the solution temperature is high. Under these conditions the measured yield of NO_3^- may be higher, while those of NO_2^- and H_2O_2 may be lower than their actual values just after bubble collapse. Since the addition of alkali was found to be effective in measuring the actual yields formed in the active bubbles, a 1.0 mM NaOH solution was used in our study.

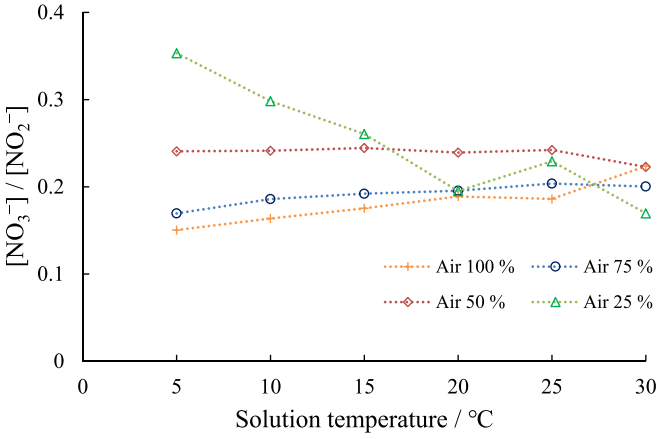

Fig. 6. Effect of solution temperature on the NO_3^-/NO_2^- ratio at different air-Ar ratio.Concentration of NaOH: 1.0 mM, sonication time: 5.0 min, ultrasonic power: 10.3 W.

3.2. *Effect of solution temperature*

Experiments were performed at different solution temperatures to discuss the chemical characteristics of the active bubbles. Fig. 2a and b show the sum of the yields of NO_2^- and NO_3^- (abbreviated as $[NO_2^-]$ +

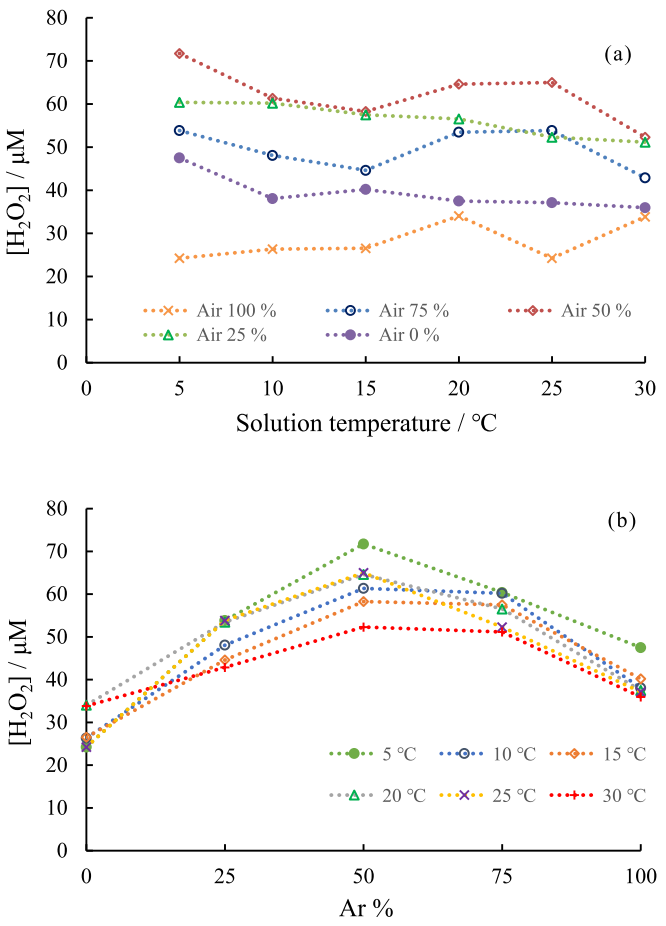

Fig. 7. (a) Effect of solution temperature on the yield of H_2O_2 at different air-Ar ratio. (b) Effect of Ar percentage in gas mixture on the yield of H_2O_2 at different solution temperature. Concentration of NaOH: 1.0 mM, sonication time: 5.0 min, ultrasonic power: 10.3 W.

$[NO_3^-]$) and ratio of $[NO_3^-]$ to $[NO_2^-]$ ($[NO_3^-]/[NO_2^-]$ ratio), respectively, as functions of the solution temperature at an ultrasonic power of 10.3 W. Because all the yields increased almost linearly with irradiation time (Supplementary data, Figs. S4–S7), we used the yields obtained at 5 min of irradiation. The experimental errors of data would be within 10% of the relative standard deviation (Supplementary data, Table S1). Fig. 2a shows that $[NO_2^-] + [NO_3^-]$ decreases with increasing solution temperature. This phenomenon is explained as follows: at higher solution temperatures, the presence of water vapor with a lower specific heat ratio within the bubbles leads to a lower bubble temperature after quasi-adiabatic collapse [37,38]. On the other hand, Fig. 2b shows that the $[NO_3^-]/[NO_2^-]$ ratio increases with an increase in the solution temperature. The similar tendency was also observed at different ultrasonic power as shown in Fig. S8. These results may be because higher solution temperatures lead to lower bubble temperatures after quasi-adiabatic collapse, thereby favoring the chemical equilibrium shift from NO formation (corresponding to NO_2^- formation) to NO_2 formation (corresponding to NO_3^- formation). This concept is consistent with that of our previous study [22], where the amounts of NO_2 and NO formed from the reaction between N_2 and O_2 were calculated using the NASA Computer Program CEA (Chemical Equilibrium with Applications) [39] under different temperature and pressure conditions. In this calculation, the $[NO_2]/[NO]$ ratio decreases when the reaction temperature increases.

Ouerhani et al. [40] investigated the yields of NO_2^- and NO_3^- formed from the sonolysis of water at 360 kHz under Ar-N_2 mixtures at 14°C and they reported that the $[NO_3^-]/[NO_2^-]$ ratio decreased with increasing N_2 %, where the increase of N_2 % in Ar-N_2 mixtures corresponds to the decrease of the maximum temperature in collapsing bubbles. The trend observed in [40] was opposite to that observed in this study. This divergence would be due to that the formation of NO_3^- and NO_2^- is affected by the amounts of O_2 inside bubbles, taking into account Eq. (5) in the Zeldovich mechanism.

3.3. *Effect of ultrasonic power*

The effect of ultrasonic power was investigated at a solution temperature of 20 °C. The results are shown in Fig. 3a and b. Fig. 3a shows that $[NO_2^-] + [NO_3^-]$ increased gradually as the ultrasonic power increased from 3.3 to 10.3 W, whereas it decreased from 10.3 to 15.0 W. The behavior of $[NO_2^-] + [NO_3^-]$ is similar to that reported in our previous study [22]. Fig. 3b shows that the $[NO_3^-]/[NO_2^-]$ ratio remains almost constant with increasing ultrasonic power. This behavior was different from that of our earlier results [22]. This divergence could be attributed to the utilization of the data obtained in the absence of NaOH. Therefore, the progress of Eq. (17) was not suppressed completely in the previous study and it is possible that the NO_2^- and NO_3^- concentrations were unintentionally measured to be lower and higher, respectively, resulting in a larger change in the $[NO_3^-]/[NO_2^-]$ ratio than in the presence of NaOH. We also previously discussed the possibility of the maximum temperature and pressure in the collapsing bubbles increasing with increasing ultrasonic power and affecting the chemical equilibrium between NO and NO_2 [22]. However, the results presented in Fig. 3b, indicating almost no changes in the $[NO_3^-]/[NO_2^-]$ ratio vs. ultrasonic powers, suggest one idea: despite the increase in ultrasonic power, the quality of the active bubbles affecting chemical reactions may not change largely.

The changes in the quality and quantity of active bubbles have been investigated under various experimental conditions. Barber et al. reported that the intensity of sonoluminescence (SL) from air single-bubble cavitation changes sensitively with water temperature [41]. When the water temperature decreases from about 35 °C to 1 °C, the intensity of SL increases about 200 times. This enhancement is suggested to be the change in the maximum bubble temperature. The intensity of SL in multi-bubble cavitation is also sensitive to the changes in the experimental parameters, although the maximum bubble temperature in multi-bubble cavitation is lower than that in single-bubble cavitation. On the other hand, in multi-bubble cavitation, the chemical effects of active bubbles would be less sensitive to the experimental parameters compared with SL. For example, it is reported that the addition of small amounts of ethanol to water decreases the intensity of SL dramatically, but it does not decrease the bubble temperature largely which was measured by the methyl radical recombination reactions [42]. Our result of Fig. 2a also indicates that the yield of NO_2^- and NO_3^- increases 3 times, when the water temperature decreases from 30 °C to 5 °C. In the case of H_2O_2 formation, the effect of the water temperature on the yield of H_2O_2 was small as shown in later (Fig. 7a). Therefore, it is suggested that the chemical effects of active bubbles may not be directly related to the phenomena of SL in some cases. This idea could be supported by Brotchie et al. [43]. They reported that the temperature requirements for sonochemiluminescence (SCL) and SL are different: SL is induced by a population of higher temperature bubbles, but SCL related to sonochemical reactions is induced by a population of relatively lower temperature bubbles [43]. They also reported that the bubble-size distributions for SL and SCL are different. Based on their report, N_2 oxidation would mainly result from active bubbles belonging to a population of relatively lower temperature bubbles. It is also reported that the population of bubble streamers increases with ultrasonic power [44] and the spatial distribution of active bubbles for SL and SCL becomes larger with ultrasonic power [44,45]. Therefore, it is probable that the number and/or size of active bubbles increasing with increasing ultrasonic power.

In the present study, when we assumed that the mean maximum temperature and pressure of active bubbles which act on N_2 oxidation

remained constant and the mean radius of these bubbles remained constant at different ultrasonic powers, it might be inferred that the increase in $[NO_2^-] + [NO_3^-]$ from 3.3 to 10.3 W is due to the increase in the number of active bubbles with higher ultrasonic powers. In multi-bubble cavitation, it is generally suggested that when the ultrasonic power (acoustic pressure amplitude) increases, "the number and/or size of active bubbles" and "the maximum temperature and pressure in the collapsing bubbles" simultaneously increase, leading to increased chemical efficiency. So far, it has been very difficult to distinguish the effects of these two factors relating to the quantity and quality, however, it may be considered in the present study that an increase in the number of active bubbles had a greater effect than an increase in the mean maximum temperature and pressure, when the ultrasonic power was increased. Furthermore, as the ultrasonic power increased from 10.3 W to 15.0 W, $[NO_2^-] + [NO_3^-]$ decreased because the number of active bubbles decreased. This is in good agreement with the results of previous papers [5,44,46]: beyond a certain ultrasonic power, the number of active bubbles decreases, resulting in a decrease in the chemical efficiency and SL intensity, owing to the formation of non-active bubbles via the occurrence of coalescence, clustering, fragmentation, and/or dissolution of active bubbles.

The results of Fig. 2b and 3b also suggest that the mean maximum temperature and pressure reached during bubble collapse is more sensitive to the change in solution temperature (from 5 °C to 30 °C) than to the change in ultrasonic power (from 3.3 W to 15.0 W). In the above discussion, we hypothesized that the mean radius of active bubbles remained constant as ultrasonic power (acoustic pressure amplitude) increased. However, Brotchie et al. [43] reported that active bubbles had the size distribution and the mean radius of active bubbles increased with increasing ultrasonic power [43]. Since it is difficult to consider the effects of the size distributions and different sizes on chemical reactions, we ignored these in our discussion. As the quantitative and qualitative effects of ultrasonic power on the chemical reactions are quite complex as described above, further research is necessary.

3.4. Effect of gas mixture and solution temperature

An aqueous solution containing a gaseous mixture of air and Ar was sonicated at different temperatures to discuss the relationship between the maximum bubble temperature (T_{max}) and N_2 oxidation. T_{max} can be estimated using the following adiabatic compression (Eq. (18)):

$$T_{max} = T_0[R_0/R_{min}]^{3(\gamma-1)}, \quad (18)$$

where T_0 is the initial temperature, R_0 is the initial bubble radius, R_{min} is the minimum bubble radius, and γ is the specific heat ratio. For example, at 15 °C, the γ value of Ar (1.668) is larger than those of N_2 (1.404), O_2 (1.401), and H_2O (1.324 at 100 °C) [47]. Considering these values, T_{max} will increase with an increasing percentage of Ar in the mixed gas bubbles.

Fig. 4a and b show the effects of solution temperature on the formation of NO_2^- and NO_3^-, respectively, at different air/Ar ratios. The yield of NO_2^- was higher than that of NO_3^- at all air/Ar ratios, and the yields of NO_2^- and NO_3^- decreased with increasing solution temperatures. As elucidated in the results depicted in Fig. 2a, this behavior can be attributed to the concurrent decrease in the bubble temperature with increasing solution temperature.

Fig. 5a and b show the yields of NO_2^- and NO_3^-, respectively, formed at the different percentages of Ar in the gas mixture. At all solution temperatures, the yield of NO_2^- and NO_3^- formed increased as the percentage of Ar increased from 0 to 25% and percentage of air decreased from 100 to 75%. This is because Ar has a higher specific heat ratio than air; when the percentage of Ar in the bubbles increased from 0 to 25%, higher temperature bubbles were generated, resulting in the progress of N_2 oxidation and effective formation of NO_2^- and NO_3^-. The gas solubility in water (ratio of mol fraction at 25 °C and 1 atm) is 0.252×10^{-4}, 0.229×10^{-4}, and 0.118×10^{-4} for Ar, O_2, and N_2, respectively [48]. As Ar has a slightly higher solubility than air, the number of active bubbles may increase as the percentage of Ar increases.

In contrast, the yield of NO_2^- and NO_3^- decreased when the percentage of Ar was greater than 25%. This could be due to the decrease in the number of N_2 and O_2 molecules in the bubbles, which made it more difficult for the N_2 oxidation to occur. Before conducting the experiment, we expected that the yield of NO_2^- and NO_3^- would reach a maximum value at an Ar percentage higher than 25%, because the higher Ar percentages contribute to the higher the bubble temperature. However, the oxidation of N_2 slowed at 50% air because of the shortage of N_2 and O_2. This result would be attributed to the extremely short reaction times which are less than ~ 0.05 μs in micrometer-sized bubbles [27]. Consequently, the insufficient reaction time may hinder the reaction progress. Based on the obtained results, equilibrium theory could not be applied to the quantitative analysis of the vapor-phase chemical reactions occurring in the bubbles. However, the equilibrium theory is important for a qualitative understanding because the characteristics of cavitation bubbles include complex phenomena.

Fig. 6 shows the effect of solution temperature on the $[NO_3^-]/[NO_2^-]$ ratio at different gas ratios. It was observed that the effect on $[NO_3^-]/[NO_2^-]$ ratio was unclear at 25 °C and 30 °C. Therefore, the tendency in the temperature range between 5 and 20 °C was focused here. At 100 and 75% air, the $[NO_3^-]/[NO_2^-]$ ratio increased with increasing solution temperature. This behavior can be attributed to the decrease in bubble temperature due to the increase in solution temperature (as discussed in Fig. 2b). However, at 50% air, the $[NO_3^-]/[NO_2^-]$ ratio remained almost constant even as the solution temperature increased. Furthermore, at 25% air, the $[NO_3^-]/[NO_2^-]$ ratio tended to decrease with increasing solution temperature. This trend was different from those observed at 100% and 75% air. This cannot be explained only by the change in the bubble temperature, as discussed in Fig. 2b. In addition, the $[NO_3^-]/[NO_2^-]$ ratio at 5 °C increased as the air ratio decreased from 100% air to 75% air, 50% air, and finally, to 25% air. Since the decrease in the air ratio (corresponding to the increase in the Ar ratio) suggests the occurrence of the increase in the maximum temperature of active bubbles, the air ratio dependence of the $[NO_3^-]/[NO_2^-]$ ratio at 5 °C also contradicts to the phenomenon observed in Fig. 2b. This reason could be because the changes in the yields of oxidants formed in the sonolysis of water affect the yields of NO_2^- and NO_3^-.

Next, we discuss N_2 oxidation from the viewpoint of the chemical reactions. As seen in Eqs. (13) and (14), the main precursors affecting the formation of HNO_2 (=NO_2^-) and HNO_3 (=NO_3^-) are considered to be NO and NO_2, respectively, where NO is formed by the oxidation of N_2 and N as shown in Eqs. (5)–(7). NO is also formed by the reaction of N with OH radicals via the extended Zeldovich mechanism (Eq. (8)). However, NO_2 is formed by the oxidation of NO as shown in Eqs. (9) and (12). Therefore, a larger amount of O_2 is required for NO_3^- formation than for NO_2^- formation. At 25% air, NO_3^- may be less likely formed because of the shortage of O_2 compared to other mixed gas ratios. While this explanation can account for some of the observed results, it cannot explain all of the results obtained here. Therefore, further discussion regarding ultrasonic cavitation is needed. For example, at a solution temperature of 5 °C, the maximum temperature in collapsing bubbles at 25% air (75% Ar) was higher than those at other mixed gas ratios. Consequently, the yields of oxidants such as OH, OOH from H (Eq. (3)), H_2O_2, and O, among others, formed during the sonolysis of water should be higher, suggesting that NO and NO_2^- oxidized to NO_2 and NO_3^-, respectively.

It has been reported that, in numerical calculations of counterflow diffusion flame, the introduction of water vapor (mass fraction of water in air = 0.05 or 0.1) to a combustion system lowers the flame temperature and partly suppresses NO formations [49]. The effect of water vapor on the chemical reactions in collapsing bubbles remains unclear. Hence, we mainly considered the effect of the specific heat ratio of water vapor and did not consider the effects of other factors in the discussion of

Fig. 2a and 2b. This is a topic for future research.

Subsequently, the yield of H_2O_2 in the sonolysis of water was investigated. The yield of H_2O_2 increased with irradiation time as seen in Fig. S9. However, it was observed that the linearity of H_2O_2 in the plot was slightly worse compared with those of NO_2^- and NO_3^-. It seems that the H_2O_2 yield was a little unstable in the presence of air. Therefore, in this study, we discuss the trends of the H_2O_2 yield under different conditions. Fig. 7a and b show the effects of the solution temperature and mixed gas ratio, respectively, on the yield of H_2O_2. As shown in Fig. 7a, the yield of H_2O_2 tended to decrease with increasing solution temperature under pure Ar atmosphere (0% air). This is because an increase in the influx of water vapor into the collapsing bubbles, resulting in a decrease in the maximum bubble temperature. It seems that the slope in Fig. 7a changes from negative to positive as the ratio of air increases. In previous studies [6,7,9,10], the solution-temperature dependence of H_2O_2 formation had a negative or positive slope. Overall, the solution-temperature dependence of H_2O_2 formation is less distinct than that of NO_3^- and NO_2^- formation. One reason for this is that the oxidants formed during the sonolysis of water reacted with N_2, N, and NO_x.

Fig. 7b shows the yield of H_2O_2 at different mixed-gas ratios. The yield of H_2O_2 reaches its maximum at 50% Ar. An appropriate amount of O_2 in an Ar system increases the yield of H_2O_2 [4,9], and the results obtained here show the same trend as those in previous studies. This is because H_2O_2 is formed from OH radicals during the sonolysis of water (Eqs. (1) and (2)) and, when O_2 is present in the reaction system, H radicals formed during the sonolysis of water react with O_2 to form OOH, which in turn produces H_2O_2 (Eqs. (3) and (4)). In the region from 50% to 100% Ar, the decrease in the yield of H_2O_2 with increasing Ar content was attributed to the decrease in the amount of O_2 in the solution, which resulted in reduced H_2O_2 formation from H radicals.

In Fig. 5a, 5b, and 7b, the maximum yield of H_2O_2 was observed at 50% Ar, but the maximum yields of NO_2^- and NO_3^- were at 25% Ar. This divergence is considered as follows: when the air percentage is lower than 75%, N_2 oxidation is less likely to occur owing to O_2 shortage. However, as the bubble temperature increased with the Ar percentage in the bubbles, water decomposition was more likely to occur. In other words, NO formation depends on O concentration, whereas H_2O_2 formation depends on OH and OOH concentrations. The experimental results at different mixed gas ratios and solution temperatures showed that the characteristics of the bubbles and chemical reactions during the collapse of the bubbles changed in a complex manner.

In this study, the sum of the yields of NO_2^- and NO_3^- was higher than that of H_2O_2. Therefore, it is useful to use the sum of the yields of NO_2^- and NO_3^- or that of NO_2^-, NO_3^-, and H_2O_2 as an indicator of the chemical effects of active bubbles. This idea is also suggested by Son and Choi [28]. We consider the NO_3^-/NO_2^- ratio and yield of NO_2^- and NO_3^- to be valuable analytical tools for understanding the characteristics and chemical effects of active bubbles. It is interesting that these values could be closely related to the quantity and quality of active bubbles.

4. Conclusions

We succeeded to measure the actual yields of NO_2^-, NO_3^-, and H_2O_2 formed just after bubble collapse, where the presence of NaOH suppressed the bulk reaction between NO_2^- and H_2O_2 during and after irradiation. It was confirmed that the yields of NO_3^- and NO_2^- decreased and NO_3^-/NO_2^- ratio increased with increasing solution temperature, suggesting that the maximum temperature in collapsing bubbles decreased with increasing solution temperature. Experiments on the effects of ultrasonic power suggested for the first time that 1) the quality of active bubbles was not largely affected by ultrasonic power, and 2) the number of active bubbles might increase with increasing ultrasonic power up to a certain power and then decreased with further ultrasonic power. This decrease was induced by the formation of non-active bubbles via the coalescence, clustering, fragmentation, and/or dissolution of active bubbles. The chemical effects of active bubbles of air/Ar gas mixtures were investigated under conditions affecting the adiabatic compression collapse of the bubbles. The yield of NO_2^- and NO_3^- was the highest at 25% Ar/75% air, and the yield of H_2O_2 was the highest at 50% Ar/50% air. When the percentage of air was less than 75%, a shortage of O_2 occurred during N_2 oxidation. In contrast, the formation of H_2O_2 proceeded more easily at 50% Ar to form various oxidants such as O, OH, and OOH. Therefore, the yield of NO_2^-, NO_3^-, and H_2O_2 was influenced by not only the maximum temperature in bubbles but also by the reactions with various oxidants. Because the sum of the yields of NO_2^- and NO_3^- was larger than that of H_2O_2, the sum or that of NO_2^-, NO_3^-, and H_2O_2 would be useful for analyzing the chemical effects of active bubbles. The NO_3^-/NO_2^- ratio could also serve as an important tool for analyzing characteristics of active bubbles.

Declaration of Competing Interest

The authors declare that they have no known competing financial interests or personal relationships that could have appeared to influence the work reported in this paper.

Data availability

Data will be made available on request.

Appendix A. Supplementary data

Supplementary data to this article can be found online at https://doi.org/10.1016/j.ultsonch.2023.106612.

References

[1] K. Makino, M.M. Mossoba, P. Riesz, Chemical Effects of Ultrasound on Aqueous Solutions. Evidence for ·OH and ·H by Spin Trapping, J. Am. Chem. Soc. 104 (1982) 3537–3539.
[2] D.B. Rajamma, S. Anandan, N.S.M. Yusof, B.G. Pollet, M. Ashokkumar, Sonochemical dosimetry: A comparative study of Weissler, Fricke and terephthalic acid methods, Ultrason. Sonochem. 72 (2021), 105413.
[3] Y. Asakura, K. Yasuda, Frequency and power dependence of the sonochemical reaction, Ultrason. Sonochem. 81 (2021) 105858.
[4] E.J. Hart, A. Henglein, Free Radical and Free Atom Reactions in the Sonolysis of Aqueous Iodide and Formate Solutions, J. Phys. Chem. 89 (20) (1985) 4342–4347.
[5] A. Henglein, M. Gutierrez, Sonochemistry and Sonoluminescence: Effects of External Pressure, J. Phys. Chem. 97 (1993) 158–162.
[6] M.H. Entezari, P. Kruus, Effect of frequency on sonochemical reactions II. Temperature and intensity effects, Ultrason. Sonochem. 3 (1) (1996) 19–24.
[7] S. Merouani, O. Hamdaoui, F. Saoudi, M. Chiha, Influence of experimental parameters on sonochemistry dosimetries: KI oxidation, Fricke reaction and H_2O_2 production, J. Hazard. Mater. 178 (2010) 1007–1014.
[8] I. Hua, M.R. Hoffmann, Optimization of Ultrasonic Irradiation as an Advanced Oxidation, Technology, Environ. Sci. Tech. 31 (8) (1997) 2237–2243.
[9] R. Pflieger, T. Chave, G. Vite, L. Jouve, S.I. Nikitenko, Effect of operational conditions on sonoluminescence and kinetics of H_2O_2 formation during the sonolysis of water in the presence of Ar/O_2, Ultrason. Sonochem. 26 (2015) 169–175.
[10] Y. Jiang, C. Petrier, T.D. Waite, Sonolysis of 4-chlorophenol in aqueous solution: Effects of substrate concentration, aqueous temperature and ultrasonic frequency, Ultrason. Sonochem. 13 (2006) 415–422.
[11] Y. Asakura, T. Nishida, T. Matsuoka, S. Koda, Effects of ultrasonic frequency and liquid height on sonochemical efficiency of large-scale sonochemical reactors, Ultrason. Sonochem. 15 (3) (2008) 244–250.
[12] A. Keck, E. Gilbert, R. Köster, Influence of particles on sonochemical reactions in aqueous solutions, Ultrason. 40 (1-8) (2002) 661–665.
[13] K. Okitsu, T. Suzuki, N. Takenaka, H. Bandow, R. Nishimura, Y. Maeda, Acoustic Multi-Bubble Cavitation in Water: A New Aspect of the Effect of Rare Gas Atmosphere on Bubble Temperature and its Relevance to Sonochemistry, J. Phys. Chem. B 110 (2006) 20081–20084.
[14] Y. Son, J. Seo, Effects of gas saturation and sparging on sonochemical oxidation activity in open and closed systems, Part I: H_2O_2 generation, Ultrason. Sonochem. 90 (2022) 106214.
[15] K. Yasuda, K. Matsuura, Y. Asakura, S. Koda, Effect of Agitation Condition on Performance of Sonochemical Reaction, Jpn. J. Appl. Phys. 48 (2009) 07GH04.
[16] Y. Kojima, Y. Asakura, G. Sugiyama, S. Koda, The effects of acoustic flow and mechanical flow on the sonochemical efficiency in a rectangular sonochemical reactor, Ultrason. Sonochem. 17 (6) (2010) 978–984.
[17] Y.i. Jiang, C. Pétrier, T.D. Waite, Effect of pH on the ultrasonic degradation of ionic aromatic compounds in aqueous solution, Ultrason. Sonochem. 9 (3) (2002) 163–168.

[18] A. Henglein, C. Kormann, Scavenging of OH Radicals Produced in the Sonolysis of Water, Int. J. Radiat. Biology 48 (1985) 251–258.
[19] M.H. Uddin, B. Nanzai, K. Okitsu, Effects of Na_2SO_4 or NaCl on sonochemical degradation of phenolic compounds in an aqueous solution under Ar: positive and negative effects induced by the presence of salts, Ultrason. Sonochem. 28 (2016) 144–149.
[20] T. Tuziuti, K. Yasui, T. Kozuka, A. Towata, Y. Iida, Enhancement of sonochemical reaction rate by addition of micrometer-sized air bubbles, Chem. A Eur. J. 110 (37) (2006) 10720–10724.
[21] D. Xia, J. Wu, K. Su, Influence of micron-sized air bubbles on sonochemical reactions in aqueous solutions exposed to combined ultrasonic irradiation and aeration processes, J. Environ. Chem. Eng. 10 (2022), 108685.
[22] K. Okitsu, Y. Itano, Formation of NO_2^- and NO_3^- in the sonolysis of water: Temperature- and pressure-dependent reactions in collapsing air bubbles, Chem. Eng. J. 427 (2022), 131517.
[23] A.I. Virtanen, N. Ellfolk, Nitrogen fixation in an ultrasonic field, J. Am. Chem. Soc. 72 (2) (1950) 1046–1047.
[24] E.L. Mead, R.G. Sutherland, R.E. Verrall, The effect of ultrasound on water in the presence of dissolved gases, Can. J. Chem. 54 (7) (1976) 1114–1120.
[25] V. Misik, P. Riesz, Nitric oxide formation by ultrasound in aqueous solution, J. Phys. Chem. 100 (1996) 17986–17994.
[26] C.A. Wakeford, R. Blackburn, P.D. Lickiss, Effect of ionic strength on the acoustic generation of nitrite, nitrate and hydrogen peroxide, Ultrason. Sonochem. 6 (3) (1999) 141–148.
[27] K. Yasui, T. Tuziuti, T. Kozuka, A. Towata, Y. Iida, Relationship between the bubble temperature and main oxidant created inside an air bubble under ultrasound, J. Chem. Phys. 127 (2007), 154502.
[28] Y. Son, J. Choi, Effects of gas saturation and sparging on sonochemical oxidation activity in open and closed systems, part II: NO_2^- /NO_3^- generation and a brief critical review, Ultrason. Sonochem. 92 (2023) 106250.
[29] K. Okitsu, A. Yue, S. Tanabe, H. Matsumoto, Y. Yobiko, Y. Yoo, Sonolytic Control of Rate of Gold(III) Reduction and Size of Formed Gold Nanoparticles in an Aqueous Solution: Relation Between Reduction Rates and Sizes of Formed Nanoparticles, Bull. Chem. Soc. Jpn 75 (2002) 2289–2296.
[30] Y. Asakura, in: Sonochemistry and the Acoustic Bubble, Elsevier, 2015, pp. 119–150.
[31] K. Yasui, Acoustic Cavitation and Bubble Dynamics, Springer, Cham, Switzerland, 2018.
[32] A.E. Alegria, Y. Lion, T. Kondo, P. Riesz, Sonolysis of aqueous surfactant solutions. Probing the interfacial region of cavitation bubbles by spin trapping, J. Phys. Chem. 93 (1989) 4908–4913.
[33] C.T. Bowman, Kinetics of nitric oxide formation in combustion processes, Symp. (Int.) Combust. 14 (1) (1973) 729–738.
[34] J.A. Miller, C.T. Bowman, Mechanism and Modeling of Nitrogen Chemistry in Combustion, Prog. Energy Combust. Sci. 15 (4) (1989) 287–338.
[35] D.E. Damschen, L.R. Martin, Aqueous Aerosol Oxidation of Nitrous Acid by O_2, O_3 and H_2O_2, Atmos. Environ. 17 (1983) 2005–2011.
[36] Kagaku-binran (1993), II-322. Ed by The Chemical Society of Japan, Maruzen, Japan.
[37] K. Yasui, Effect of liquid temperature on sonoluminescence, Phys. Rev. E 64 (2001), 016310.
[38] K. Okitsu, I. Kurisaka, B. Nanzai, N. Takenaka, H. Bandow, Sonochemistry of aqueous $NaAuCl_4$ solutions with C3–C6 alcohols under a noble gas atmosphere, Ultrason. Sonochem. 41 (2018) 397–403.
[39] S. Gordon, B.J. McBride, Computer Program for Calculation of Complex Chemical Equilibrium Compositions and Applications, NASA Reference, Publication (1996) 1311.
[40] T. Ouerhani, R. Pflieger, W.B. Messaoud, S.I. Nikitenko, Spectroscopy of Sonoluminescence and Sonochemistry in Water Saturated with N_2−Ar Mixtures, J. Phys. Chem. B 119 (2015) 15885–15891.
[41] B.P. Barber, C.C. Wu, R. Löfstedt, P.H. Roberts, S.J. Putterman, Sensitivity of sonoluminescence to experimental parameters, Phys. Rev. Lett. 72 (9) (1994) 1380–1383.
[42] M. Ashokkumar, F. Grieser, A Comparison between Multibubble Sonoluminescence Intensity and the Temperature within Cavitation Bubbles, J. Am. Chem. Soc. 127 (2005) 5326–5327.
[43] A. Brotchie, F. Grieser, M. Ashokkumar, Effect of power and frequency on bubble-size distributions in acoustic cavitation, Phys. Rev. Lett. PRL 102 (2009), 084302.
[44] H.-B. Lee, P.-K. Choi, Acoustic power dependences of sonoluminescence and bubble dynamics, Ultrason. Sonochem. 21 (6) (2014) 2037–2043.
[45] M. Ashokumar, J. Lee, Y. Iida, K. Yasui, T. Kozuka, T. Tuziuti, A. Towata, Spatial Distribution of Acoustic Cavitation Bubbles at Different Ultrasound Frequencies, Chem. Phys. Chem. 11 (2010) 1680–1684.
[46] S.-I. Hatanaka, K. Yasui, T. Kozuka, T. Tuziuti, H. Mitome, Influence of bubble clustering on multibubble sonoluminescence, Ultrason. 40 (1-8) (2002) 655–660.
[47] Kagaku-binran (1993), II-234-235. Ed by The Chemical Society of Japan, Maruzen, Japan.
[48] Kagaku-binran (1993), II-156-157. Ed by The Chemical Society of Japan, Maruzen, Japan.
[49] D. Zhao, H.Yamashita, T. Yamamoto, T. Furuhata, N. Arai, Consideration of chemical kinetics on mechanism of NO_x reduction by steam addition, Kagaku Kogaku Ronbunshu 25 (1999) 955–960.